Thermomechanical Characterization of Oleogels elaborated with a Low Molecular Weight Ethyl Cellulose and Monoglycerides

Martha Laura García-Ortega
Universidad Autónoma de San Luis Potosí
Maria Eugenia Charó-Alvarado
Universidad Autónoma de San Luis Potosí
Jaime David Pérez-Martínez
Universidad Autónoma de San Luis Potosí
Jorge Fernando Toro-Vazquez (toro@uaslp.mx)
Universidad Autónoma de San Luis Potosí

Research Article

Keywords: Ethly cellulose, Monoglycerides, Oleogels, Glass transition temperature

Posted Date: December 6th, 2023

DOI: https://doi.org/10.21203/rs.3.rs-3576058/v1

Additional Declarations: No competing interests reported.

Abstract

The interaction between a low molecular weight (i.e., 19 kDa) ethyl cellulose (EC) and a commercial monoglyceride (MGc) in the development of EC-MGc oleogels was evaluated through rheological, DSC, and infrared spectroscopy measurements. The oleogels were developed through cooling (80°C to 2°C, 10°C/min) vegetal oil solutions of mixtures of EC at concentrations above (10%), below (7%), and at its minimal gelling concentration (8%), with MGc concentrations below its minimal gelling concentration (0%, 0.1%, 0.25%, 0.5%, 1%). At 0.10% MGc most of the monoglycerides developed hydrogen bonds with the EC. Thus, the EC-0.10% MGc oleogels were structured through EC-monoglyceride-EC interactions, that as the EC concentration increased entrapped the oil providing higher elasticity (G') than the EC oleogels. At MGc concentrations ≥ 0.25% the higher relative polarity of the oil favored the EC-EC interactions over the EC-monoglyceride-EC interactions. At temperatures < 10°C the monoglycerides in the oil crystallized within the free spaces of the entangled EC fibers acting as active filler. Thus, at the same EC concentration the EC-0.25% MGc, EC-0.50% MGc, and EC-1% MGc oleogels achieved higher G' than the corresponding EC-0.10% MGc oleogels ($P < 0.01$). This behavior was more evident as the EC concentration increased. Additionally, the rheological measurements during cooling showed that below 40°C the EC went through a structural rearrangement that decreased the oleogels' elasticity. Since the structural rearrangement was cooling rate, EC and MGc concentration dependent, these factors could be used to tailor the rheological properties of oleogels developed with low molecular weight EC.

1. Introduction

The structuring of vegetable oils without the use of saturated and *trans* fatty acids is essential for the food industry that nowadays faces the challenge of incorporating healthy edible oils in food products. Currently, structuring vegetable oils through molecular self-assembly of edible gelators is a relevant research area not only from the fundamental perspective, but also from the practical/technological point of view. Among the most studied edible low molecular weight molecules that develop self-standing structures in vegetable oils (i.e., oleogels) are the phytosterols [1–3], lecithin [4, 5], monoglycerides [6, 7], and also *n*-alkanes, long chain esters, fatty acids and alcohols in pure state [8–11] or as native complex mixtures present in candelilla, carnauba, rice bran, and sunflower waxes [12–19]. On the other hand, just a few high molecular weight edible molecules are capable of gelling edible oils, i.e., ethyl cellulose (EC), chitin, and chitosan [20–23]. Of these edible polymers, the self-assembly behavior of EC in vegetable oils is the most studied [20, 22, 24, 25].

The EC is a linear polysaccharide derived from cellulose, and therefore, formed by 1, 4-β-D-glucose units. The EC is produced through the ethoxylation of the OH groups present in the glucose monomer at carbons 2, 3, or 6 [22, 26]. The extent of ethoxylation, known as the substitution degree (SD), determines the EC's solubility profile. Thus, EC with a SD between 1.0 and 1.5 is water-soluble while solubility in organic solvents, including vegetable oils, is achieved with a SD between 2.4 and 2.5. [21, 27]. The EC is in the list of food additives approved by the European Union (Annex II to Regulation (EC) No 1333/2008) as *"Additives other than colors and sweeteners,"* [28] and has the GRAS status granted by the Food and

Drug Administration (21CFR Sec. 172.868) [29, 30]. The use of EC to gel edible oils require the initial solubilization of EC in the oil, commonly achieved by heating an EC-oil dispersion to temperatures above the polymer glass transition followed by cooling to room temperature. Within this context, Davidovich-Pinhas, Barbut, and Marangoni reported that the glass transition temperature increased from 115°C to 130°C the EC's molecular weight increased from 19 kDa to 144 kDa [31]. Unfortunately, the use of high temperatures to achieve EC's solubilization might trigger oxidation reactions in the oil, particularly in those oils with high extent of unsaturation.

Several authors have reported that surfactants molecules (e.g., monoglycerides, sorbitan esters, and fatty acids) added during preparation of EC oleogels, act as plasticizers interacting at the junction zones of the polymer causing the chains to fall apart at certain places and glide over each other [25, 32, 33]. The use of plasticizer results in an increase of the free volume, a reduction in the EC's glass transition temperature [34], and subsequently in a modification of the elastic [25, 34–37] and thixothropic [38] properties of the EC oleogels. Research done by López-Martínez et al. [24] compared the thermo-mechanical properties and storage stability of monoglyceride oleogels with and without EC. These authors reported that the EC delayed the monoglyceride polymorphic transitions and the syneresis usually present in monoglyceride oleogels [24]. The authors proposed that during the development of oleogels there is a monoglyceride-EC interaction through the OH groups of each molecule [24]. The monoglyceride-EC interaction was also observed in a gelled W/O emulsion (Gelled-W/O-E) formulated with glycerol monostearate, EC and 20% water [39]. In the Gelled-W/O-E the elasticity and time involved in the monoglyceride polymorphic transition, significantly increased as the glycerol monostearate concentration went from 0.5–1%. Additionally, the Gelled-W/O-E system showed higher rheological properties when compared with those of a conventional W/O emulsion and oleogels developed with the same amount of glycerol monostearate (no EC added) and EC (no glycerol monostearate added) [39]. Within this context, an additional study showed that mixed oleogels developed with EC, monoglycerides and candelilla wax had 100% elasticity recovery after shearing, and rheological behavior like the one obtained with commercial shortenings [40]. This phenomenon was associated by the authors with a tentative formation of an EC interchain hydrogen bonding mediated by the OH groups of the monoglycerides [40]. We need a better understanding of the interactions between EC and surfactant molecules to tailor EC oleogels with particular rheological properties.

Within the previous framework, in the present work we studied the thermo-mechanical properties and microstructure of oleogels made by mixtures of EC and monoglyceride in the vegetable oil, using concentrations above and below the EC minimal gelling concentration. Previous studies done by different research groups used EC with molecular weights above 28 kDa, providing viscosities equal to or greater than 10 cP. This as measured under standard conditions (i.e., at 25°C in an 80:20 toluene:ethanol solution with 5% wt/wt EC) [20, 22, 25, 26, 37, 41]. The use of EC with molecular weight lower than 28 kDa would provide lower viscosities and, subsequently olegels with lower elastic properties. Within this framework in the present work, we used an EC with a reported molecular weight of 19 kDa [31] that, under standard measurements conditions provide a viscosity (i.e., 4 cP) lower than the one provided by EC used in other studies [20, 22, 25, 26, 37, 41]. The use of the 4 cP EC would allow us to assess better the effect of the

monoglycerides on the rheological behavior of the EC during the oleogel development. Particularly when using low monoglyceride concentrations (i.e., below the minimal gelling concentration), as in the present study. The analytical techniques to characterize the EC-monoglyceride systems were differential scanning calorimetry, oscillatory rheology, infrared spectroscopy, and visible light microscopy. Most of the studies done with EC oleogels describe their rheological profile while cooling just until achieving 50°C or 60°C [22, 25, 42]. In other cases, the rheological measurements were done under isothermal conditions (i.e., 40°C, 30°, 25°C) after initially setting the EC oleogel at 25°C for about 8 h [43], or during heating (5°C/min) from 25°C to 80°C previously developed EC olegels [44]. Thus, as an additional contribution of the present study we monitored the rheological properties of EC and EC-monoglyceride oil solutions as temperature decreased until achieving 2°C (i.e., during oleogelation). There is limited information regarding the rheological changes occurring during oleogelation of vegetable oil with EC or EC-monoglyceride mixtures.

2. Materials and Methodologies

2.1. Materials

The monoglyceride used was a commercial food grade additive (MGc) provided by Palsgaard Industri de Mexico (product code 0093). Based on previous analysis [7] the monoglyceride was constituted by 37.7% (± 0.1%) of 1-glycerol monostearate, 54.0% (± 0.0%) of 1-glycerol monopalmitate, 7.5% (± 0.0%) free fatty acids, and 0.8% (± 0.1%) of moisture. The EC was obtained from Sigma Aldrich (Oakville, ON, Canada; CAS Number 9004-57-3). According to the manufacturer the EC had a SD of 2.5 and, under standard conditions (i.e., 25°C in an 80:20 toluene:ethanol solution with 5% EC), provide a viscosity of 4 cP.

2.2. Gelling properties of the EC, MGc, and EC-MGc mixtures in the vegetable oil

2.2.1. Determination of the minimal gelling concentration

We prepared EC vegetable oil solutions between 2% and 10% (wt/wt) at 1% interval in 100 mL glass beakers. The proper amount of EC was slowly added to the preheated vegetable oil (160°C) and mixed by intermittent gently stirring during 30 min. Afterwards, 6 g of the EC-vegetable oil solution were transferred to PYREX glass test tubes (2 cm i.d. X 12.5 cm) preheated to 80°C. The tubes with the EC-vegetable oil solution were kept at 80°C for 15 min in a temperature-controlled oil bath and then transferred into a refrigerated chamber set at 2°C. After 3 h within the refrigerated chamber (2°C), the minimal gelling concentration was determined as the lowest EC concentration at which we observed slow or no flow after inverting the test tubes for 30 min at 2°C. In the same way, after preparing 0.10–4% (w/w) MGc vegetable oil solutions, we determined the MGc minimal gelling concentration at 2°C. However, in this case the MGc was dissolved in the oil at 80°C by gently stirring for 15 min. This temperature limited the monoglyceride isomerization commonly occurring at higher temperatures [45].

2.2.2. Mixed EC-MGc oleogels

Based on the results obtained from the determination of the minimal gelling concentration, we developed EC-MGc oleogels using factorial combinations of EC (0%, 7%, 8%, and 10%, w/w) and MGc (0%, 0.10%, 0.25%, 0.5%, 1.0%, and 2.0%, w/w) concentrations prepared as described as described for the determination of the minimal gelling concentration evaluating the gelling/no-gelling behavior of the EC-MGc systems at 2°C Under the same conditions we evaluated the gelling/no-gelling behavior of EC (no MGc added) and MGc (no EC added) vegetable oil solutions (i.e., control systems).

2.3. Thermal analysis by differential scanning calorimetry

2.3.1. Glass transition temperature of the EC

The glass transition temperature (Tg) of the EC was determined in a differential scanning calorimeter (DSC) equipment (Discovery Series, TA Instruments, New Castle, USA) set in modulated mode using nitrogen as purge gas (50 mL/min). Approximately 10 mg of neat EC hermetically sealed in Tzero aluminum pans were placed in the thermocell and equilibrated for 2 min at 25°C. Afterwards, the system was heated at 3°C/min until reaching 245°C (first heating stage). After 2 minutes at this temperature, we cooled the system at 10°C/min until reaching 2°C and after 2 min again heated (3°C/min) until reaching 245°C (second heating stage). The heating and cooling cycles stages were applied with an amplitude of ± 1°C applied in periods of 60 seconds. Using the TRIOS software (V 3.2.0.3877; TA Instruments, New Castle, USA) we determined the Tg analyzing the heat flow data from the second heating stage (3°C/min). The mean and corresponding standard deviation of Tg was obtained from two independent determinations (n = 2).

2.3.2. Thermal analysis of EC, MGc, and EC-MGc oleogels

Approximately 6 mg of the corresponding EC-MGc, EC and MGc oil solutions were sealed in Tzero aluminum pans and heated for 15 min at 80°C, and then cooled at 10°C/min until reaching 2°C. The cooling thermograms of the different systems were analyzed using the Universal Analysis 2000 software (Version 4.5A, TA Instruments New Castle, DE, USA). For each of the EC-MGc and control systems we obtained at least two independent determinations (n = 2).

2.4. Infrared spectroscopy of the EC-MGc oleogels

The analysis was done using a Bruker infrared spectrometer model Vertex 70 (Bruker Optics, Billerica, MA, USA) coupled to a Hyperion 2000IR microscope (Bruker Optics, Billerica, MA, USA) equipped with a heating/cooling stage (Linkam T95, Linkam, Surey, UK) and a temperature control stage (LTS 350, relinked Scientific Instruments). Freshly prepared EC-MGc, EC or MGc solutions, as previously described, were allowed to cool. Once achieving 80°C a small sample was placed on a $BaCl_2$ sample window previously set in the stage (80°C). The cover $BaCl_2$ slide (80°C) was placed on the top of the sample, and after 15 min at 80°C the system was cooled to 2°C at 10°C/min. The infrared spectra of the EC-MGc, EC or MGc systems were obtained (32 scans) at 80°C and 2°C in transmission mode using a 15X objective. The spectra were analyzed using the Opus 7.2 software (Bruker Optics, Billerica, MA). With the same

spectrometer we obtained the infrared spectra of the EC and MGc powders using the ATR sample holder accessory.

2.5. Rheology measurements of the mixed EC-MGc oleogels

We evaluated the rheological properties of the EC-MGc systems and the corresponding EC and MGc controls using an MCR 301 rheometer (Paar Physica, Stuttgart, Germany), equipped with a sand-blasted steel plate-plate geometry (PP50 50 mm diameter) and a true-gap system. The temperature was controlled with a Peltier temperature control located on the base of the geometry and with a Peltier-controlled hood (H-PTD 200). The equipment was controlled through the software Start Rheoplus US200/32 version 2.65 (Anton Paar, Graz, Austria). A sample of the corresponding solution preheated at 80°C was applied on the base of the geometry pre-set at 80°C and then, using the true gap function, the plate of the geometry was set on the sample surface. While keeping the temperature at 80°C the sample was subjected to a low shear rate ($\approx 10\ s^{-1}$) for 15 min, and then under quiescent conditions the system was cooled at 10°C/min until achieving 2°C. The elastic (G') and loss (G") modulus were measured during cooling always applying conditions within the linear viscoelastic region (LVR) of the system. The LVR conditions were previously determined from strain (γ) sweeps obtained over the entire temperature interval (80°C to 2°C) applying a frequency (*f*) of 1 Hz. Additionally, keeping conditions always within the LVR, we determined the *f* sweeps of the EC and the EC-MGc systems from 100 Hz to 0.01 Hz applying, depending on the sample, a γ between 0.02% and 0.08%.

2.6. Visible light microscopy.

We obtained visible light microphotographs of the EC-MGc systems and the corresponding EC and MGc controls using an Olympus BX51 microscope (Olympus Optical Co., Ltd., Tokyo, Japan) equipped with a color video camera (KPD50; Hitachi Digital, Tokyo, Japan) and a heating/cooling stage (LTS 350, Linkam Scientific Instruments, Ltd.) connected to a liquid nitrogen tank and to a temperature control station (TP94, Linkam Scientific Instruments, Ltd., Surrey, England). A sample of the corresponding melted solution (80°C) was spread on a slide using another glass slide placed at a 45° angle. Both glass slides were previously heated to 80°C. The slide with the sample was placed on the microscope stage previously set at 80°C, and after 15 min at this temperature, the system was cooled at 10°C/min until achieving 2°C. To visualize the EC fibers in the oleogels we did not use a coverslip. This was because the EC fibers and the glass have similar refractive indexes [46].

2.7. Statistical analysis

The effect of the treatment conditions on the different properties evaluated in the EC-MGc oleogels and control systems was analyzed through ANOVA and contrast between the treatment means using the STATISTICA V 12 (StatSoft Inc., Tulsa, OK).

3. Results and discussion

3.1 Thermal behavior of the EC

Figure 1 shows the thermograms for the reversing and non-reversible components of the heat flow obtained from the first and second heating stages of the 4cP EC. The reversing signal measures the heat capacity associated with the Tg and the melting, while the non-reversing signal contained the heat flow of kinetic events like crystallization and crystal perfection (i.e., annealing or aging). Within this context, from the reversing signal obtained during the first heating stage we determined the Tg value (Fig. 1A). The exotherm starting just above Tg in the non-reversing heat flow thermogram showed the relaxation enthalpy associated with stress relaxation events of the EC (Fig. 1A). The relaxation enthalpy corresponds to the stress released upon heating polymers, like the EC, and its magnitude depends on the time the material was stored at a temperature below Tg (i.e., aging or annealing) [47, 48]. The transition associated with Tg was more evident in the reversing signal obtained during the second heating stage (Fig. 1B). The non-reversing heat flow thermogram of the second heating stage did not show any relaxation exotherm above Tg because, after previous cooling to 2°C, the EC sample was immediately heated (i.e., no aging or annealing stage occurred). It is important to note that the Tg values determined from the reversing signal of the first and second heating stages were statistically the same ($P < 0.01$). These results contrast with the Tg values determined by Davidovich-Pinhas, Barbut, and Marangoni [31] in a similar 4 cP EC using standard DSC. These authors reported Tg values of ≈ 127°C and ≈ 115°C obtained from the first and second heating stages, respectively [31]. Our results showed that during the first heating stage, the glass transitions and relaxation endotherm occurred very close. This would make difficult to get reliable Tg measurements through standard DSC. Therefore, in the absence of modulated DSC equipment is advisable to determine the Tg of the EC using the heat flow thermogram just from the second heating stage, i.e., after releasing the EC molecular stress and corresponding relaxation enthalpy. On the other hand, above the end of the exotherm corresponding to the relaxation enthalpy, the reversing heat flow of the first heating showed two endotherms, a small one with a peak temperature at 156.2°C (± 0.3°C) (i.e., T_{M1}) and a larger one with a peak temperature at 225.4°C (± 0.05°C) (i.e., T_{M2}; Fig. 1A). Both endotherms, each associated to melting events of the EC molecules, were more evident in the reversing heat flow from the second heating. The T_{M1} and T_{M2} from the second heating were 153.1°C (± 0.7°C) and 226.4°C (± 1.6°C) (Fig. 1B). The T_{M1} form the first heating was about 3.1°C higher than the corresponding T_{M1} value from the second heating ($P < 0.05$), a thermal behavior like the one previously reported by Davidovich-Pinhas, Barbut, and Marangoni for an EC 4 cP [31]. However, in that study the T_{M1} values from the first and second heating obtained using standard DSC were ≈ 168°C and ≈ 165°C, respectively. Unfortunately, in that study the heating of the EC was just up to 200°C and consequently the higher temperature endotherm (i.e., corresponding to T_{M2}) was not observed [31]. This high temperature endotherm could be associated with the thermal decomposition of EC. However, based on the thermograms behavior obtained after the first and second heating, it was evident that the EC had a thermo-reversible behavior, i.e., no thermal decomposition of the EC occurred. Thus, the T_{M2} and corresponding melting heat (i.e., ΔH_M) from the first ($\Delta H_M = 225.4 \pm 0.05$ J/g) and second heating ($\Delta H_M = 226.4 \pm 1.58$ J/g) were statistically the same. It is well known that polymeric materials like EC have

molecular weight polydispersity. Therefore, we considered that the high melting temperature endotherm was associated with a high molecular fraction (i.e., high melting temperature fraction) of the EC.

3.2. Cooling thermograms of the EC-MGc system

Based on the results of the gelling/non-gelling evaluation we considered that the minimal gelling concentration for the EC and the MGc in the vegetable oil were 8% and 2% (w/w), respectively. At 8% EC we obtained a weak gel that during the time of the evaluation slowly flowed over the test tube walls, while at 2% MGc we obtained a self-supporting structure (Table 1). Below these concentrations we obtained just high viscosity fluids. Within this framework we evaluated the gelling/non-gelling behavior of EC-MGc vegetable oil solutions formulated by mixing EC concentrations equal, above, and below 8% EC with MGc concentrations lower and equal to 2%. The results obtained showed (Table 1) that the interaction between the EC and the MGc resulted in the development of a self/supporting structure (i.e., an oleogel). This tentative synergistic interaction between the EC and the MGc was particularly evident when the 7% EC was mixed with 0.25–1.0% of MGc (i.e., below the minima gelling concentration of EC and MGc) and when the 8% EC was mixed with MGc concentrations of 0.1% and above. This was because when the 7% EC and the 0.25–1.0% of MGc solutions were used independently did not gel, but in mixture the systems developed well-structured gels (Table 1). Similarly, the 8% EC system developed a week gel but in mixture with 0.10–1% MGc (i.e., MGc concentrations below its minimal gelling concentration) formed well-structured gels (i.e., oleogels) (Table 1).

The Figs. 2 to 4 show the cooling thermograms for the 7%, 8%, and 10% EC and the 2%, 1%, and 0.5% MGc vegetable oil solutions, in comparison with the cooling thermograms for the corresponding EC-MGc mixtures. The thermograms just show the temperature interval where the monoglyceride's transitions occurred (i.e., 40°C to 2°C interval). Evidently the thermograms for the EC vegetable oil solutions did not show any phase transition that could be associated with the self-assembly of EC molecules. This, in spite the 10% and 8% EC oil solutions developed well-structured and weak gels, respectively (Table 1). Similar results had been reported by other authors with 12–15% (w/w) of 10 cP, 20 cP, 45 cP, and 100 cP EC solutions in canola oil [22]. Possibly, the gelation mechanisms followed by the EC in the vegetable oil did not involve the development of highly ordered secondary and three-dimensional microstructures. Subsequently, the formation of a self-supporting structure by the EC in the vegetable oil did not release sufficient energy to be detected by DSC. The thermal transitions during oleogelation and subsequent melting of EC in oil solutions are poorly understood. In contrast, the monoglycerides' transitions in the vegetable oil are better characterized. Thus, upon cooling the initial molecular self-assembly of the monoglycerides resulted in the formation of a bilayer organization (i.e., the Lα phase) stabilized through hydrogen bonds established through the primary and secondary OH groups of the monoglycerides. Upon further cooling, the aliphatic chains crystallize developing the sub-α phase. It is well-known that the isotropic phase to Lα transition temperature is concentration dependent, occurring at lower temperature as the monoglyceride concentration in the oil solution decreased. On the other hand, the temperature for the Lα to sub-α phase transition is independent of the monoglyceride concentration and depends only on the number of carbons of the esterified fatty acid [6, 7, 49]. Within this framework, the cooling

thermograms showed that the 2% MGc was the only control system that showed the Lα and sub-α phase transitions (Figs. 2A, 3A, and 4A), and the only MGc control that developed a self-supporting structure (Table 1). The cooling thermograms for the 1% and 0.5% MGc controls just showed the development of the Lα phase (Figs. 2B, 2C, 3B, 3C, 4B, 4C), but the 0.25% and 0.10% MGc controls did not show any phase transition (results not shown). Additional experiments showed that in the 0.10% and 0.25% MGc control systems the exotherm corresponding to the Lα phase occurred below 2°C (i.e., at 0.65°C in the 0.25% MGc control). Because in the present study the thermograms were obtained just until achieving 2°C (Figs. 2 to 4), the Lα and the sub-α exotherms were not observed in the 0.10% and 0.25% MGc thermograms. These results agreed with the phase transition behavior recently reported by Charó-Alvarado et al. [49] for neat 1-glycerol monostearate and neat 1-glycerol monopalmitate in vegetable oil, both major components of the MGc used in the present study. According to these authors, at monoglyceride concentrations lower than 2%, the Lα phase crystallizes concomitantly with the sub-α1 phase developing just one small exotherm at lower temperature than when the Lα and the sub-α transitions occur independently (i.e., monoglyceride concentrations above 2%) [49]. In spite of the crystallization behavior of the MGc, it was interesting to note that some EC-MGc mixtures formulated with 0.25% and 0.10% of MGc (i.e., 8% EC-0.25%, MGc, 8% EC-0.1% MGc, 7% EC-0.25% MGc) developed well-structured oleogels (Table 1). These results indicated that the tentative synergistic EC-MGc interaction occurred independent of the crystallization of the monoglycerides (i.e., in the vegetable oil solution).

Table 1. Gelling/non-gelling behavior at 2°C of mixtures of ethyl cellulose (EC) and commercial monoglyceride (MGc).

	MGc (% wt/wt)					
EC (% wt/wt)	0	0.10	0.25	0.50	1	2
0	-	No gelling	No gelling	No gelling	No gelling	Gel*
7	Non gelling	Non gelling	Gel	Gel	Gel	Gel
8	The gel slowly flowed over the test tube walls*	Gel	Gel	Gel	Gel	Gel
10	Gel	Gel	Gel	Gel	Gel	Gel

* Minimal gelling concentration of the EC or the MGc

3.2.1 Determination of the free and interacting monoglycerides after oleogelation of the EC-MGc systems

We observed that the onset temperature for the Lα phase crystallization (T_{Cr-O}) in the MGc control systems decreased as the MGc concentration decreased from 2–0.5% (Figs. 2 to 4). This behavior has been previously observed with vegetable oil solutions of commercial and pure monoglycerides [7, 49]. In the same way, independent of the EC concentration used, the cooling thermograms for the EC-2% MGc, EC-1% MGc, and EC-0.5% MGc showed that the T_{Cr-O} associated to the crystallization exotherm for the Lα phase followed similar behavior (Figs. 2 to 4). However, in the EC-MGc systems the crystallization exotherm for the Lα phase was smaller and occurred at a lower T_{Cr-O} than the one observed in the corresponding MGc control. These results were explained considering that during cooling and subsequent oleogelation of the EC-MGc systems, some OH groups of the EC developed hydrogen bonds with the primary and secondary OH groups of the monoglyceride. This would result in a decrease of the monoglyceride concentration in the oil phase. Consequently, the monoglyceride remaining in the oil phase of the EC-MGc systems (i.e., considered free monoglyceride) would crystallize in the Lα phase at a lower T_{Cr-O} than the one observed in the corresponding MGc control. As an example, the T_{Cr-O} for the controls

with 2%, 1% and 0.5% MGc were ≈ 32°C, ≈ 22.5°C and ≈ 11°C, respectively. In contrast, in the 7% EC-2% MGc, 7% EC-1% MGc, and 7% EC-0.5% MGc the T_{Cr-O} for the Lα exotherm occurred at ≈ 29°C, ≈ 19.5°C and ≈ 8.5°C, respectively. Similar behavior was observed for lauric acid in 20 cP EC oleogels [42]. However, in that study the authors considered that the EC had a steric hindrance effect during the lauric acid crystallization, thus shifting its crystallization to lower temperatures [42]. Based on the previous discussion, using 0.25–2% MGc vegetable oil solutions we determined the regression equation of the T_{Cr-O} for the Lα transition on the corresponding MGc concentration. Although the T_{Cr-O} of the 0.25% MGc oil solution occurred at a temperature lower than 2°C, its value was included in the determination of the regression equation. The corresponding plot and associated quadratic regression equation are shown in the Fig. 5. Note that for the regression analysis the MGc concentration was expressed as Moles of monoglyceride in the oil. The determination coefficient (R^2) of the equation ($R^2 = 0.978$; $P < 0.001$) indicated that the quadratic effect of the monoglyceride concentration explained ≈ 98% of the T_{Cr-O} behavior in the oil solutions. Using the regression equation (Fig. 5) and the T_{Cr-O} determined in the EC-MGc systems with 0.25%, 0.5% or 1% of MGc, we estimated the corresponding Moles of monoglycerides in the oil phase (i.e., the Moles of free monoglycerides). Then, by subtracting the Moles of free monoglycerides from the total number of Moles of monoglycerides present in the corresponding EC-MGc system, we calculated the Moles of monoglycerides interacting/g of EC. Finally, assuming that the 4 cP EC used in the study had the molecular weight of 19 kD reported in [31], we calculated the Moles of interacting and free monoglycerides per Mole of EC and evaluated their behavior as a function of the EC and MGc concentration (Fig. 6). Within this context, the results shown in Fig. 6A indicated that during oleogelation the concentration of interacting monoglycerides/Mole of EC followed a curvilinear behavior as a function of the EC concentration. This behaviour showed a tendency to achieve a maximum value at 8% EC (i.e., the minimum gelling concentration). However, in the EC-MGc systems with 0.5% and 1% MGc the effect of the EC on the amount of interacting monoglycerides was not statistically significant. In these EC-MGc systems the Moles of interacting monoglycerides/Mole of EC essentially depended on the monoglycerides concentration in the system. Thus, in the EC-0.5% MGc oleogels the Moles of interacting monoglycerides/Mole of EC was 0.79 (± 0.16), and in the EC-1% MGc oleogels was 1.58 (± 0.20) Moles of interacting monoglycerides/Mole of EC. These results were achieved independent of the concentration of EC. In contrast, the EC-2% MGc system observed a significant quadratic behavior of the Moles of interacting monoglycerides/Mole of EC achieving a maximum at 8% EC and a minimum at 10% EC ($P < 0.005$; Fig. 6A). These results indicated that above the minimal gelling concentration for the EC, the self-assembly between EC molecules was favored over the EC-monoglyceride interaction. This behavior was more evident as the MGc concentration increased in the EC-MGc system (Fig. 6A). In contrast, the behavior of the Moles of free monoglycerides/Mole of EC (Fig. 6B) showed that, independently of the MGc concentration, the amount of free monoglycerides decreased as the EC concentration increased ($P < 0.001$). Evidently, these results showed that for the same percentage of MGc in the EC-MGc system, as the EC concentration increased the lower the concentration of free monoglycerides. Nevertheless, it was evident that the EC effect on the free monoglyceride concentration was lower as the percentage of MGc in the EC-MGc system decreased. This since the slope of the linear regression equation of the Moles of free

monoglycerides/Mole of EC on the EC concentration became less negative the lower the MGc concentration in the EC-MGc system (i.e., the linear slope was − 1.40 for the EC-2% MGc, -0.80 for the EC-1% MGc, and − 0.49 for the EC-0.5% MGc; $P < 0.01$, Fig. 6B). Based on these results we would expect that the slope of the linear regression equation of the Moles of free monoglycerides/Mole of EC on the EC concentration would approach a zero value in the EC-0.25% MGc system and, particularly in the EC-0.1% MGc system. Therefore, the concentration of free monoglycerides in the oil phase would be negligible or approaching a zero value in the EC-0.25% MGc system and, particularly in the EC-0.1% MGc system. Unfortunately, as already indicated, we could not determine the T_{Cr-O} in the EC-0.25% MGc and in the EC-0.1% MGc systems and consequently we could not evaluate the EC effect on the free and interacting monoglycerides at these low MGc concentrations. The results show in Fig. 6B indicated that for the same concentration of EC, a higher amount of free monoglyceride remained in the oil phase as the MGc concentration increased in the EC-MGc system. The free monoglycerides would modify the polarity of the vegetable oil affecting the solubility of the EC in the oil. Additionally, the free monoglycerides at temperatures below their T_{Cr-O} could crystallize as micelles or lamellas, potentially acting as active filler of the fibrillar network developed by the EC. Based on the previous discussion, we considered that in the EC-0.25% MGc and, particularly, in the EC-0.1% MGc system the monoglycerides' effect on the oil relative polarity and their tentative crystallization below their T_{Cr-O} would be negligible. This because most if not all the monoglyceride would be interacting with the EC through hydrogen bonds developed between the OH groups of the monoglycerides and the OH groups of the EC (i.e., inter-hydrogen bonds).

3.3. EC-MGc interactions through infrared measurements

The Fig. 1SI (Supportive Information) shows the infrared spectra for the EC (Fig. 1SI panel A) and the MGc (Fig. 1SI panel B) powders as received from the manufacturers. The infrared spectra of the powder EC showed two strong bands in the 2960 cm^{-1} to 2830 cm^{-1} interval, associated to the asymmetric and symmetric stretching vibrations of the acyl CH_2 groups of EC as reported by Reddy, Nagoji, and Sahoo [50]. The broad peaks observed between 3250^{-1} cm^{-1} and 3650 cm^{-1} were associated to the "polymeric" bonded OH stretch [51]. The infrared spectra of the powder MGc was like the one shown by another commercial monoglyceride (i.e., Dimodan) of similar composition to the MGc used in the present study [52]. The most relevant information obtained was that the powder MGc did not show any transmittance band in the interval, between 3650 cm^{-1} and 3550 cm^{-1}, signals associated to the primary and secondary OH groups stretch [51]. These results indicated that in the solid state the primary and secondary OH groups of the MGc were already developing hydrogen bonds between monoglyceride molecules, changing the OH groups' intensity to a lower frequency. Consequently, the infrared spectra of the powder MGc showed a broad dimeric band with peaks at 3305 cm^{-1} and at 3242 cm^{-1} associated to the stretch of hydrogen bonded OH groups (i.e., intermolecular hydrogen bonds). Figure 2SI shows the infrared spectra for the vegetable oil, the 7% EC and the 1% MGc control systems, and the corresponding 7% EC–1% MGc mixture measured at 80°C in the oil (Fig. 2SI panel A), and at 2°C in the EC-MGc oleogels (Fig. 2SI panel B). The spectrums are shown just between 3200 cm^{-1} and 3750 cm^{-1}, mainly because this interval includes the bands associated to the functional groups tentatively involved in the EC-MGc

interaction. We noted that at 80°C and 2°C the vegetable oil showed a broad band between 3425 cm^{-1} and 3525 cm^{-1} (Fig. 2A-SI). This band was present also in the oil before the heating treatment to solubilize the EC, and therefore could not be associated to oil oxidation because of the heat applied. This band was associated to the OH stretch of the antioxidant used by the vegetable oil manufacturer (i.e., TBHQ) and with the presence of minor native phenolic components of the oil (i.e., tocopherols and phytosterols) [53]. Unfortunately, this oil's band occurred within the wavenumber interval associated to the polymeric bonded OH stretch of the EC (i.e., the 3250^{-1} cm^{-1} to 3650 cm^{-1} interval) [51] observed, independent of the measurement temperature, in the 7% EC control system and in the 7% EC-1% MGc mixture (Fig. 2-SI). This overlap of bands limited the assessment of the interaction between the hydrogen bonded OH groups of the EC with the OH groups of the MGc. Nevertheless, by comparing the 1% MGc and the 7% EC-1% MGc spectrums measured at 80°C and at 2°C (Fig. 2SI) we corroborated that during oleogelation of the EC-MGc mixtures, the OH of the MGc and the hydrogen bonded OH groups of the EC interacted developing hydrogen bonds. Thus, at 80°C the 1% MGc control system and the 7% EC-1% MGc system showed a broad transmittance band in the interval associated to the primary and secondary OH groups stretch i.e., between 3650 cm^{-1} and 3550 cm^{-1} [51]. However, in the 7% EC-1% MGc system the band was observed as a shoulder of the transmittance band corresponding to the polymeric bonded OH stretch of the EC (i.e., the 3250^{-1} cm^{-1} to 3650 cm^{-1} band) (Fig. 2SI panel A). These results indicated that at 80°C the primary and secondary OH groups of the MGc were free, and consequently at this temperature no evident interaction occurred between the MGc and the EC. Once the temperature decreased to 2°C, the band associated to the primary and secondary OH groups stretch of the monoglycerides disappeared from the 1% MGc and the 7% EC-1% MGc spectrums. We observed similar infrared spectrum behavior in the EC-MGc systems containing 8% and 10% of EC and 2% of MGc (results not shown). However, in the EC-MGc systems using MGc concentrations lower than 0.5% (i.e., 0.25% and 0.10%) the infrared signal for the OH stretch of the MGc was not detected.

3.4. Rheological behavior of the EC vegetable oil solutions during cooling

The G' profile during cooling of the 7%, 8%, and 10% EC vegetable oil solutions are shown in Fig. 7. Previous studies observed that during cooling of vegetable oil solutions of EC10, EC 20, EC45, and EC100 the temperature where G' became greater than G" (i.e., the cross-over temperature) occurred below 140°C [22, 25]. According to these observations our results showed that, independent of the EC concentration, from the beginning of the rheological measurements at 80°C the G' was higher than the G" and this behavior continued until achieving 2°C (data not shown). Within this context, during cooling the G' of the 7%, 8%, and 10% EC systems showed a concomitant increment until achieving a plateau between 50°C and 40°C (Fig. 7). With the G' values at the plateau we calculated the mean elasticity between 50°C and 40°C and the corresponding standard deviation for the 7%, 8%, and the 10% EC systems. The resulting mean G' were 861 ± 32.7 Pa, 918.3 ± 54.4 Pa, and 1024.1 ± 15.4 Pa, for the 7%, 8%, and the 10% EC systems, respectively. These G' values were significantly different ($P < 0.05$) and showed a direct linear increment as function of the EC concentration ($R^2 = 0.81$, $P < 0.005$). Studies done with EC vegetable oil

solutions cooled up to 60°C using low cooling rates (i.e., 1°C/min, 3°C/min, or 5°C/min) achieved higher G' values than when using higher cooling rates (i.e., 10°C/min) [22]. According to this study the cooling rate effect on G' was evident just in EC of low molecular weights (i.e., 10 cP EC and 20 cP EC with tentative molecular weights of 29.6 kD and 51.9 kD, respectively). This since the cooling rate effect on G' was not observed in the oleogels developed with EC of molecular weights of 72.8 kD and 81.3 kD (i.e., 45 cP EC and 100 cP EC, respectively) [22, 31]. These results showed that low molecular weight EC cooled at rates lower than 10°C/min achieved better structural arrangements that resulted in oleogels with higher G'. Although the 4 cP EC used in the present study had a reported molecular weight of 19 kD [31], we just did some preliminary experiments to evaluate the cooling rate effect in the EC 4 cP rheology (*vide infra*).

As cooling continued below 40°C, the rheological profile of the 7% and 8% EC oleogels showed a decrease in G' followed by an increase after 10°C until achieving 2°C (Fig. 7). The decrease in G' was higher in the 7% EC system (i.e., the EC solution that did not gel) than in the 8% EC system (i.e., the EC solution that developed a weak gel) (see Table 1). Additionally, we observed that the G' of the 7% and 8% EC systems after attaining 2°C was lower than the corresponding G' achieved at the 50°C to 40°C plateau ($P < 0.05$; Fig. 7). This was particularly evident in the 7% EC system. In contrast, the 10% EC oleogels (i.e., the EC solution that developed a well-structured gel; Table 1) did not show an evident G' decrease after achieving 40°C (Fig. 7). These results indicated that below 40°C until achieving 2°C, the 4cP EC went through a concentration dependent structural rearrangement directly associated with the capacity of the EC to develop a gel above a particular concentration. However, this structural rearrangement was not a thermodynamic transition because the corresponding thermograms did not show thermal transitions in the temperature interval studied (Figs. 2 to 4). This rheological behavior of the EC in vegetable oil solutions has not been reported previously, probably because most rheological studies had been done during cooling just until achieving 50°C or 60°C [22, 25, 42] or during heating from 25°C to 80°C previously developed olegels with EC of higher molecular weight [44]. The rheological profile during cooling of the 4 cP EC oil solutions at the minimal gelling concentration and below (i.e., 8% and 7%, respectively), suggested that the inter-hydrogen bonds between EC fibers were not enough to withstand the structural rearrangement of the EC molecules that tentatively occurred below 40°C. Subsequently, at the minimal gelling concentration and below the EC microstructure went through a partial (i.e., 8% EC) or significative (i.e., 7% EC) collapse resulting in a decrease in the oleogel's elasticity. This phenomenon occurred unless we used higher EC concentration (i.e., 10%) or achieved higher supercooling (i.e., a temperature lower than 20°C) that assured the formation of the hydrogen bonds between EC fibers (Fig. 7). Thus, at 10% the EC developed a well-structured network and, subsequently below 40°C the oleogels' elasticity remained constant. Thus, the G' for the 10% EC for the 50°C to 2°C interval had a value significantly equal to the one achieved at the 50°C to 40°C plateau (i.e., 1024.1 ± 15.4 Pa; Fig. 7). In contrast, the 7% and 8% EC systems required temperatures below 10°C to achieve the supercooling required to develop the hydrogen bonds between the EC fibers. The result was that at 2°C the 7% and 8% EC systems achieved G' values of 440.5 ± 72.8 Pa and 823.0 ± 134.4 Pa, respectively. However, these G' values were lower than the elasticity achieved by 7% and 8% EC systems at the 50°C to 40°C plateau (i.e., 861 ± 32.7 Pa, 918.3 ± 54.4 Pa, respectively; $P < 0.01$), previous to the tentative structural rearrangement

of the EC that occurred below 40°C. Within this context, it is important to note that we did some preliminary experiments to study the cooling rate effect on the tentative EC structural rearrangement associated with the G' decrease observed below 40°C. Thus, the decrease in G' observed in the 4 cP EC oil solutions using a cooling rate of 10°C/min, was limited or not present at all when using lower cooling rates (i.e., i.e., below 5°C/min). Additionally, according to the results obtained by Davidovich-Pinhas, Barbut, and Marangoni [22], the 4cp EC oleogels obtained at lower cooling rates achieved higher G' values than the ones obtained at 10°C/min. This behavior was observed even in the 7% EC oil solution (results not shown). These preliminary results indicate that the tentative structural rearrangement of the 4 cP EC occurring below 40°C, was concentration dependent but also cooling rate dependent. This concentration and cooling rate structural rearrangement of the EC could be used to tailor the rheological properties of the EC oleogels.

The *f* sweeps for the 7%, 8%, and 10% EC systems at 2°C are shown in the Fig. 3SI. The use of an *f* sweep is particularly useful to study the relationship between the microstructure of systems (i.e., oleogels) with their viscoelastic properties. Frequency sweeps give information about the colloidal forces and the extent of particle-to-particle interactions (i.e., EC fibers in an oleogel) involved in the rheological behavior at high frequencies (i.e., fast motion conditions on short timescales) and low frequencies (i.e., slow motion conditions on long timescales or at near equilibrium conditions). The *f* sweeps of the 7% and 8% EC (Fig. 3SI panels A and B, respectively) systems showed that, under near equilibrium conditions (i.e., at frequencies lower than 10 Hz), conditions close to those occurring while inverting the test tubes during 30 min at 2°C, the elastic properties of the EC microstructure dominated. In other words, within this *f* interval the response to stress of the 7% and 8% EC systems was essentially elastic and independent of the frequency (Fig. 3SI panels A and B). However, above *f* = 10 Hz (i.e., as time scale became shorter) the G' of the 7% EC system became frequency-dependent, even showing a tendency to achieve a crossover point (i.e., an *f* value where G' was equal to G"; Fig. 3SI panel A). The *f* value at the crossover point is inversely associated with the stress relaxation time of the microstructure under measurement [54]. Then, the 7% EC system showed finite stress relaxation times and, therefore, a tendency for phase separation as a function of time. In contrast, the 10% EC system showed a frequency independent behavior for the whole *f* interval (Fig. 3SI panel C). Thus, in the 10% EC oleogel (Fig. 3SI panel C) the oil phase remained trapped within the EC's three-dimensional microstructure under near equilibrium and short time scale conditions. Consequently, the behavior of the *f* sweeps agreed with the results shown in Table 1, i.e., at 7% EC we developed a sol, at 8% the EC developed a gel-like structure, and at 10% the EC developed a true gel.

3.5. Rheological behavior of the EC-MGc vegetable oil solutions during cooling

Figure 8 shows the G' profile during cooling of the EC-0.10% MGc (Fig. 8A), EC-0.25% MGc (Fig. 8B), EC-0.50% MGc (Fig. 8C), and EC-1.0% MGc (Fig. 8D) systems at the different EC concentrations studied. Figure 9 shows photographs of the microstructure corresponding to the oleogels at 2°C, and the corresponding *f* sweeps are shown in Figs. 4SI to 7SI. Overall, the photographs showed the microfibrillar structure of the EC with some areas showing birefringence. The EC birefringence seems to arise from

remanent semi-crystalline regions of the cellulose fibers separated by amorphous regions [55]. Considering the G' profile during cooling of the EC systems (Fig. 7), the monoglycerides had an effect in the rheology of the EC-MGc systems particularly evident, independent of the EC concentration, at temperatures below 50°C (Fig. 8). Thus, the significant decrease in G' observed in the 7% and 8% EC systems below 50°C (Fig. 7), was practically absent in the rheological profile of the 7% EC-0.10% MGc and 8% EC-0.10% MGc systems (Fig. 8A). Nevertheless, we still observed below 30°C a small decrease in G' which was followed by an increase below 15°C, until G' achieved a plateau between 8°C and 2°C. The G' mean value for this temperature interval was 1081.3 ± 19.3 Pa and 1425 ± 27.4 Pa for the 7% EC-0.10% MGc and the 8% EC-0.10% MGc systems, respectively. These G' values were significantly higher ($P < 0.001$) than the G' achieved at 2°C just by the 7% and 8% EC. In contrast, the 10% EC-0.1% MGc showed an exponential increase in the elasticity from 80°C until achieving ≈ 8°C followed by a G' plateau until attaining 2°C. The addition of 0.10% MGc and subsequent crystallization ought to increase the solid content of the system contributing to the oleogels' elasticity. However, after applying the same time-temperature conditions as for the EC-MGc systems, the G' of 0.1% MGc oil solutions measured at 2°C was too low and impossible to measure (data not shown). Therefore, the contribution of the 0.1% MGc to the rheology of the EC-0.1% MGc systems was negligible. Within this context, the addition of 0.1% MGc to 7% EC resulted in a significant increase in the G' (2°C) from 440.5 ± 72.8 Pa in the 7% EC system up to 1081.3 ± 19.3 Pa in the 7% EC-0.10% MGc system ($P < 0.05$). Nevertheless, the 7% EC-0.10% MGc system did not develop a self-supporting structure (Table 1). In contrast, at 2°C the 8% EC developed a weak gel with a G' of 823.0 ± 134.4 Pa, while the 8% EC-0.10% MGc developed a self-supporting structure with a significantly higher G' (1425 ± 27.4 Pa; $P < 0.01$). The 10% EC developed a gel at 2°C (Table 1) with a G' of 1023.9 ± 46.6 Pa, an elasticity value significantly lower to the one achieved by the 10% EC-0.10% MGc (4895 ± 63.5 Pa; $P < 0.05$). These results showed that the rheological behavior of the EC-0.1% MGc oleogels was determined through a synergistic interaction between the monoglycerides and the EC. Additionally, we noted that the difference between the G' of the EC oleogels with that achieved by the EC-0.1% MGc was larger as the EC concentration increased. Therefore, the synergistic interaction between the 0.1% MGc and the EC was higher as the EC concentration increased. Within this framework, the 7% EC-0.1% MGc, 8% EC-0.1% MGc, and the 10% EC-0.1% MGc systems showed a denser fibrillar microstructure than that developed just by the EC (Fig. 9). A phenomenon that was more evident as the EC concentration increased. As previously discussed, we considered that at this low MGc concentration (i.e., 0.10%) most of the monoglyceride interacted with the OH groups of different EC chains (i.e., inter-hydrogen bonds). Thus, in the EC-0.10% MGc systems the EC-monoglyceride-EC interaction increased the free space between EC chains. The overall result was a more efficient oil physical entrapment throughout the EC-monoglyceride-EC microfibrillar structure, and therefore higher G' in contrast with the one achieved just by the EC. Despite the higher elasticity obtained with the EC-0.10% MGc oleogels, the *f* sweeps of these systems (Fig. 4SI) showed limited difference with the rheological behavior observed by the EC systems (Fig. 3SI). For instance, in contrast with the *f* sweeps obtained with the 7% and 8% EC systems (Fig. 3SI panels A and B) the ones obtained with the 7% EC-0.10% MGc and the 8% EC-0.10% MGc showed a crossover point above 20 Hz (Fig. 4SI panels A and B). Consequently, applying stress at high *f* (i.e., above 20 Hz) to the 7% EC-0.10% MGc and the 8% EC-0.10% systems, the EC-monoglyceride-EC

chains glide over each other resulting in the flow of the oleogels. In contrast, applying stress under near equilibrium conditions (i.e., below 20 Hz) the 7% EC-0.10% MGc and the 8% EC-0.10% systems showed a frequency independent behavior (Fig. 4SI panels A and B), behaving as a gel similar to the rheological behavior observed by the corresponding EC system (Fig. 3SI panels A and B). In the same way, the 10% EC-0.10% MGc oleogels showed an independent elastic behavior in the whole frequency interval (Fig. 4SI panel C), similar to the rheological behavior observed by the 10% EC oleogels (Fig. 3SI panel C).

The EC mixed with MGc concentrations 2.5, 5 and 10 times higher than the one used in the EC-0.10% MGc systems, resulted in a different rheological behavior (Figs. 8B, 8C, and 8D). At these MGc concentrations the 7% and 8% EC systems again showed the decrease in G' observed below 40°C. However, as cooling continued achieving temperatures between 25°C and 15°C the EC with 0.25%, 0.50%, and 1.0% MGc showed an incipient G' increment followed by a decrease (Figs. 8B to 8D). This rheological behavior, particularly evident in the 7% and 8% EC with 0.5% MGc and 1% MGc systems, occurred just before observing a major elasticity increment (Figs. 8C and 8D). According to the thermograms shown in Figs. 2 to 4, the Lα phase crystallized in the 0.5% and the 1% MGc control systems at a T_{Cr-O} of ≈ 11°C and ≈ 22.5°C, respectively. Therefore, we associated this rheological behavior with the onset of crystallization in the Lα phase of the free monoglycerides with the subsequent development of a solid phase. We considered that the heat of crystallization associated with the monoglycerides' nucleation, resulted in the melting of the incipient solid phase with the consequent decrease in G'. As cooling proceeded the system achieved enough supercooling to produce the massive crystallization of the free monoglycerides resulting in the major increase in G' (Figs. 8C and 8D). As already discussed, the concentration of free monoglycerides in the EC-0.25% MGc was low resulting in a T_{Cr-O} below 2°C. Therefore, in the EC-0.25% systems the crystallization effect of the free monoglycerides on the G' profile was not that evident (Fig. 8B). Thus, although the elasticity of the EC-0.25% MGc oleogels was significantly higher than the achieved by the EC-0.1% MGc systems, the f sweeps of both systems were similar (contrast Figs. 4SI and 5SI). Within this context, it is important to point out that the G' achieved at 2°C by the 0.25%, 0.50%, and 1% MGc oil solutions were lower than 60 Pa. Therefore, considering the G' achieved at 2°C just by the EC, it was evident that the EC and the monoglycerides had in the EC-MGc systems a synergistic interaction resulting in oleogels of higher elasticity. Thus, the G' (2°C) achieved by the EC-0.25% MGc, the EC-0.5% MGc, and the EC-1% oleogels varied from 680 ± 36.80 Pa, with the 7% EC-0.25%, up to 18700 ± 2500.2 Pa with the 10% EC-1% MGc. We explained these results considering that above T_{Cr-O} the monoglycerides in the oil phase (i.e., free monoglycerides), present in the EC-0.25% MGc, the EC-0.5% MGc, and the EC-1% MGc systems, ought to increase the relative polarity of the oil tentatively favoring the EC-EC interactions (i.e., decreasing the EC solubility in the vegetable oil). Additionally, once achieving temperatures below T_{Cr-O} the free monoglycerides crystallized within the free spaces of the entangled EC fibers providing an active filler effect. Thus, in contrast with the microstructure developed just by the EC, in the presence of MGc at concentrations above 0.25% the EC microfibrillar organization would be additionally structured by the free monoglycerides crystallized within the free spaces of the entangled EC fibers. Within this context, Fig. 9 shows that the 7% EC-1% MGc, the 8% EC-1% MGc, and the 10% EC-1% MGc developed a denser fibrillar microstructure than the one developed just by the EC.

Unfortunately, through visible light microscopy the monoglyceride crystal appeared as small dark acicular or cuneiform crystals making difficult to differentiate from the EC fibrillar microstructure (Fig. 8SI). Additionally, with visible light microscopy we were not able to detect monoglyceride crystals below 0.5% MGc concentration. Finally, in contrast with the *f* sweep behavior observed by the EC systems (Fig. 3SI), independent of the EC concentration the EC-0.5% MGc (Fig. 6SI) and the EC-1% MGc (Fig. 7SI) oleogels showed a frequency independent rheological behavior. We noted that in the EC-0.5% MGc oleogels, and particularly in the EC-1% MGc oleogels, the G' increased as f decreased (Figs. 6SI and 7SI). Because the *f* sweeps were determined going from high (100 Hz) to low (0.01 Hz) frequencies, the increase in G' as *f* decreased was associated to the monoglyceride crystallization occurring during the rheological measurement under isothermal conditions (2°C). Regardless this, the frequency independent rheological behavior of the EC-0.5% MGc and the EC-1% MGc oleogels was evident (Figs. 6SI and 7SI).

3.6. Conclusions

The results of this study present clear evidence that using a cooling rate of 10°C/min, low molecular weight EC (i.e., 4 cP EC) can develop well-structured oleogels through its interaction with MGc essentially through two mechanisms. At MGc below 0.25% (i.e., 0.10%) most of the monoglycerides interacted with the OH groups of different EC chains, resulting in oleogels structured by EC-monoglyceride-EC interactions established through inter-hydrogen bonds. At the cooling rate used the EC at the minimal gelling concentration (8%) and below (7%) went through a structural rearrangement at temperatures below 40°C that resulted in a decrease in the oleogels' elasticity (Fig. 7). Nevertheless, in the presence of 0.1% MGc the EC structural rearrangement was limited or eliminated, tentatively because the EC-monoglyceride-EC interactions stabilized the EC structure during cooling. The overall result was that the EC-monoglyceride-EC microstructural organization provided an efficient oil physical entrapment developing oleogels with higher G' in contrast with the G' achieved by the oleogels structured just through EC-EC interactions. This effect was more evident the higher the EC concentration, mainly because the EC structural rearrangement observed below 40°C occurred in lower extent the higher the EC concentration. It is important to note that at 0.10% MGc the synergistic EC-MGc interaction occurred in the absence of the monoglyceride crystallization. This contrasted with the EC-MGc interaction occurring at MGc concentrations ≥ 0.25%. We considered that as the MGc concentrations increased in the EC-MGc systems, the oil's relative polarity decreased the EC solubility decreased favoring the EC-EC interactions over the EC-monoglyceride-EC interactions. At these MGc concentration conditions, once we achieved temperatures < 10°C the monoglycerides in the oil phase crystallized within the free spaces of the entangled EC fibers acting as active filler. The overall result was that, for the same EC concentration the EC-0.25% MGc, EC-0.50% MGc, and EC-1% oleogels achieved higher G' than the corresponding EC oleogels, and even higher than the EC-0.10% MGc oleogels (Figs. 7 and 8). This behavior was more evident as the EC concentration increased. Ongoing studies indicated that the EC structural rearrangement observed below 40°C through G' measurements was not present when using lower cooling rates (i.e., 3°C/min). This EC structural rearrangement might be associated with the lower G' observed by other authors in EC oleogels obtained using high cooing rates (i.e.,10°C/min) and low molecular weight

EC [22]. Therefore, since the EC structural rearrangement was cooling rate, EC and MGc concentration dependent, these factors could be used to develop well-structured oleogels with designed rheological properties using low molecular weight EC. It is important to note that the results here discussed, were obtained using oil solutions of EC-MGc mixtures formulated with EC concentrations above, below and at its minimal gelling concentrations, and with MGc concentrations below its minimal gelling concentration. This is pointed out because most studies done by different authors utilized monoglyceride concentrations well above the corresponding minimal gelling concentration. Based on our results, the rheology of these systems would dependent essentially on the monoglyceride crystallization, increasing the potential deleterious effect of the sub-α to β polymorphic transition on the oleogels microstructure and oil-binding. Within this context, previous research by our group observed that, in comparison with oleogels developed just by monoglicerides, in EC-monoglyceride oleogels the sub-α to β polymorphic transition and the subsequent β crystals' agglomeration was delayed during 14 days of storage at 15°C [24]. Evidently the study of the factors that determine the EC-monoglyceride interaction (i.e., molecular weight of EC, type and concentration of monoglycerides) will result in the design of new types of oleogels with useful physical and functional properties.

Declarations

Conflict of interest

The authors declare that they have no conflict of interest.

Data transparency/availability

All data and materials that support the published claims are available upon request. The software used for statistical analysis supports the published claims and comply with field standards.

Funding declaration

The present research was supported by Consejo Nacional de Ciencia y Tecnología (CONACYT) through the grant CB-280981-2018. M. L., Garcia-Ortega greatly appreciates the scholarship provided by CONACYT to conclude her Ph.D. program.

Author contributions

M. L. García-Ortega was a Ph. D. student, and these results are part of her thesis research. She was closely involved in the DSC and rheological measurements as well with the microscopy studies reported in this manuscript. M. E. Charó-Alvarado was involved in the determination and interpretation of the infrared spectra. J. D. Pérez-Martínez was mainly involved in the interpretation of the rheograms. J. F. Toro-Vazquez was the project and research group leader, study conception and design, also acting as M. L., García-Ortega thesis advisor. The first draft of the manuscript was written by J. F. Toro-Vazquez and all authors contributed and commented on further versions of the manuscript. All authors read and approved the final manuscript.

References

1. A. Bot, W. G. M. Agterof, J. Am. Oil Chem. Soc. (2006) https://doi.org/10.1007/s11746-006-1234-7
2. A. Bot, R. Den Adel, E. C. Roijers, J. Am. Oil Chem. Soc. (2008) https://doi.org/10.1007/s11746-008-1298-7
3. R. Den Adel, P. C. M. Heussen, A. Bot, J. Phys. Conf. Ser. (2010) doi:10.1088/1742-6596/247/1/012025
4. L. Han, L. Li, B. Li, L. Zhao, G. Q. Liu, X. Liu , X. Wang, J. Am. Oil Chem. Soc. (2014) https://doi.org/10.1007/s11746-014-2526-y
5. M. Martínez-Ávila, A. De la Peña-Gil, F. M. Álvarez-Mitre, M. A. Charó-Alonso, J. F. Toro-Vazquez, J. Am. Oil Chem. Soc. (2019) https://doi.org/10.1002/aocs.12188
6. C. H. Chen, I. Van Damme, E. M. Terentjev, Soft Matter (2009) https://doi.org/10.1039/B813216J
7. A. López-Martínez, J. A. Morales-Rueda, E. Dibildox-Alvarado, M. A. Charó-Alonso, A. G. Marangoni, J. F. Toro-Vazquez, Food Res. Int. (2014) https://doi.org/10.1016/j.foodres.2014.08.029
8. F. G. Gandolfo, A. Bot, E. Flöter, J. Am. Oil Chem. Soc.(2004) https://doi.org/10.1007/s11746-004-0851-5
9. J. A. Morales-Rueda, E. Dibildox-Alvarado, M. A. Charó-Alonso, R. G. Weiss, J. F. Toro-Vazquez, Eur. J. Lipid Sci. Technol. (2009) https://doi.org/10.1002/ejlt.200810174
10. R. S. H. Lam, M. A. Rogers, Cryst. Growth Des. (2011) https://doi.org/10.1021/cg200553t
11. S. S. Sagiri, B. Behera, R. R. Rafanan, C. Bhattacharya, K. Pal, I. Banerjee, D. Rousseau, Soft Mater. (2014) https://doi.org/10.1080/1539445X.2012.756016
12. L. S. K. Dassanayake, D. R. Kodali, S. Ueno, K. Sato, J. Am. Oil Chem. Soc. (2009) https://doi.org/10.1007/s11746-009-1464-6
13. F. M. Alvarez-Mitre, J. A. Morales-Rueda, E. Dibildox-Alvarado, M. A. Charó-Alonso, J. F. Toro-Vazquez, Food Res. Int. (2012) https://doi.org/10.1016/j.foodres.2012.08.025
14. A. I. Blake, J. F. Toro-Vazquez, H.-S. Hwang in Edible Oleogels, ed. By A. G. Marangoni, N. Garti (Elsevier, 2018) p.133
15. H.S. Hwang, S. Kim, M. Singh, J. K. Winkler-Moser, S. X. Liu, J. Am. Oil Chem. Soc. (2012) https://doi.org/10.1007/s11746-011-1953-2
16. J. F. Toro-Vazquez, J. A. Morales-Rueda, E. Dibildox-Alvarado, M. Charó-Alonso, M. Alonzo-Macias, M. M. González-Chávez, J. Am. Oil Chem. Soc. (2007) https://doi.org/10.1007/s11746-007-1139-0
17. J. F. Toro-Vazquez, R. Mauricio-Pérez, M. M. González-Chávez, M. Sánchez-Becerril, J. J. Ornelas-Paz, J. D. Pérez-Martínez, Food Res. Int. (2013) https://doi.org/10.1016/j.foodres.2013.09.046
18. M. Chopin-Doroteo, J. A. Morales-Rueda, E. Dibildox-Alvarado, M. A. Charó-Alonso, A. de la Peña-Gil, J. F. Toro-Vazquez, Food Biophys. (2011) https://doi.org/10.1007/s11483-011-9212-5
19. A. R. Patel, M. Babaahmadi, A. Lesaffer, K. Dewettinck, J. Agric. Food Chem. (2015) https://doi.org/10.1021/acs.jafc.5b01548

20. A. K. Zetzl, A. G. Marangoni, S. Barbut, Food Funct. (2012) doi: 10.1039/c2fo10202a
21. W. Koch, Ind. Eng. Chem. (1937) https://doi.org/10.1021/ie50330a020
22. M. Davidovich-Pinhas, S. Barbut, A. G. Marangoni, Carbohydr. Polym. (2015) https://doi.org/10.1016/j.carbpol.2014.10.035
23. J. M. Milani, M. H. Naeli, in Handbook of Chitin and Chitosan, ed. By S. Gopi, S. Thomas, A. Pius (Elsevier, 2020), pp. 383-406
24. A. López-Martínez, M. A. Charó-Alonso, A. G. Marangoni, J. F. Toro-Vazquez, Food Res. Int. (2015) https://doi.org/10.1016/j.foodres.2015.03.019
25. M. Davidovich-Pinhas, S. Barbut , A. G. Marangoni, Carbohydr. Polym. (2015) https://doi.org/10.1016/j.carbpol.2015.03.085
26. T. Laredo, S. Barbut, A. G. Marangoni. Soft Matter (2011) https://doi.org/10.1039/C0SM00885K
27. S. Guo, M. Lv, Y. Chen, T. Hou, Y. Zhang, Z. Huang, Y. Cao, M. Rogers, Y. Lan, Food Funct. (2020) https://doi.org/10.1039/C9FO02540E
28. COMMISSION REGULATION (EU) No 1129/2011 of 11 November 2011 amending Annex II to Regulation (EC) No 1333/2008 of the European Parliament and of the Council by establishing a Union list of food additives. (Publications Office of the European Union). https://op.europa.eu/en/publication-detail/-/publication/28cb4a37-b40e-11e3-86f9-01aa75ed71a1
29. GRAS Notices GRN No. 470 Ethyl cellulose (U.S. Food and Drug Administration, Last Updated: 04/06/2023), https://www.cfsanappsexternal.fda.gov/scripts/fdcc/index.cfm?set=GRASNotices&id=470
30. CFR - Code of Federal Regulations Title 21 (U.S. Food and Drug Administration, Last Updated: 01/17/2023), https://www.accessdata.fda.gov/scripts/cdrh/cfdocs/cfCFR/CFRSearch.cfm?fr=172.868
31. M. Davidovich-Pinhas, S. Barbut, A. G. Marangoni, Cellulose (2014) https://doi.org/10.1007/s10570-014-0377-1
32. A. Haj Eisa, S. Laufer, J. Rosen-Kligvasser, M. Davidovich-Pinhas, Eur. J. Lipid Sci. Technol. (2020) https://doi.org/10.1002/ejlt.201900044
33. A. G. Marangoni, in Fat Crystal Networks, ed. By A. G. Marangoni (Marcel Dekker, New York, NY, USA, 2005), pp. 21–82.
34. T. Dey, D. A. Kim, A. G. Marangoni, in Edible Oleogels Structure and Health Implications, ed. By A.G. Marangoni, N. Garti (AOCS Press, Urbana, Illinois, 2011), pp.295-311
35. R. Hyppölä, I. Husson, F. Sundholm, Int. J. Pharm. (1996) https://doi.org/10.1016/0378-5173(96)04436-5
36. A. G. Marangoni, Chocolate compositions containing ethylcellulose. (United States Patent Application Publication, 2012) https://patents.google.com/patent/US20120183651A1/en17
37. A. K. Zetzl, A.J. Gravelle, M. Kurylowicz, J. Dutcher, S. Barbut, A. G. Marangoni, Food Struct. (2014) https://doi.org/10.1016/j.foostr.2014.07.002

38. T. A. Stortz, A. G. Marangoni, **Green Chem.** (2014) https://doi.org/10.1039/C4GC00052H
39. M.L. García-Ortega, J.F. Toro-Vazquez ,S. Ghosh, Food Res. Int. (2021) https://doi.org/10.1016/j.foodres.2021.110763
40. A. K. Rodríguez-Hernández, J. D. Pérez-Martínez, J. A. Gallegos-Infante, J. F. Toro-Vazquez, J. J. Ornelas-Paz, Carbohydr. Polym. (2021) https://doi.org/10.1016/j.carbpol.2020.117171
41. A. J. Gravelle, S. Barbut, A. G. Marangoni, Food Funct. (2013) https://doi.org/10.1039/C2FO30227F
42. A. Haj Eisa, S, Laufer, J. Rosen-Kligvasser, M. Davidovich-Pinhas, Eur. J. Lipid Sci. Technol. (2019) https://doi.org/10.1002/ejlt.201900044
43. M. Davidovich-Pinhas, A. J. Gravelle, S. Barbut, A. G. Marangoni, Food Hydrocoll. (2015) https://doi.org/10.1016/j.foodhyd.2014.12.030
44. J. Gómez-Estaca, A. M. Herrero, B. Herranz, M. D. Álvarez, F. Jiménez-Colmenero, S. Cofrades, Food Hydrocoll. (2019) https://doi.org/10.1016/j.foodhyd.2018.09.029
45. A. Watanabe, J. Amer. Oil Chem. Soc. (1997) https://doi.org/10.1007/s11746-997-0079-z
46. L.W. McKeen, in Film Properties of Plastics and Elastomers, ed. By L.W. McKeen (Elsevier, 2012), pp. 353-378.
47. D. Cangialosi, in Handbook of Thermal Analysis and Calorimetry, ed. By S. Vyazovkin, N. Koga, C. Schick (Elsevier Science B.V., 2018) pp. 301-337, https://doi.org/10.1016/B978-0-444-64062-8.00013-9)
48. N. Guigo, N. Sbirrazzuoli, in Handbook of Thermal Analysis and Calorimetry, ed. By S. Vyazovkin, N. Koga, C. Schick (Elsevier Science B.V., 2018) pp. 399-429, https://doi.org/10.1016/B978-0-444-64062-8.00002-4.
49. M. E., Charó-Alvarado, M. A. Charó-Alonso, A. de la Peña-Gil, J. F. Toro-Vazquez, Food Biophys. (2023) https://doi.org/10.1007/s11483-023-09799-2
50. B. B. K. Reddy, K. E. V. Nagoji, S. Sahoo, J. Pharm. Sci. (2018) http://dx.doi.org/10.1590/s2175-97902018000317277
51. J. Coates, in Encyclopedia of Analytical Chemistry, ed. By R.A. Meyers (John Wiley & Sons Ltd, Chichester, 2000), pp 10815–10837
52. M. Mionić Ebersold, M. Petrović, W.-K. Fong, D. Bonvin, H. Hofmann, I. Milošević, *Nanomaterials* (2018) https://doi.org/10.3390/nano8020091
53. Y.B. Che Man, W. Ammawath, M.E.S. Mirghani, Food Chem. (2005) https://doi.org/10.1016/j.foodchem.2004.05.059
54. T. G. Mezger, The Rheology Handbook, 4th ed. (Vincentz Network, Hanover, Germany, 2014).
55. S.P. Gautam, P.S. Bundela, A.K. Pandey, Jamaluddin Jamaluddin, M.K. Awasthi, S. Sarsaiya, J. Appl. Nat. Sci. (2010) https://doi.org/10.31018/jans.v2i2.143

Figures

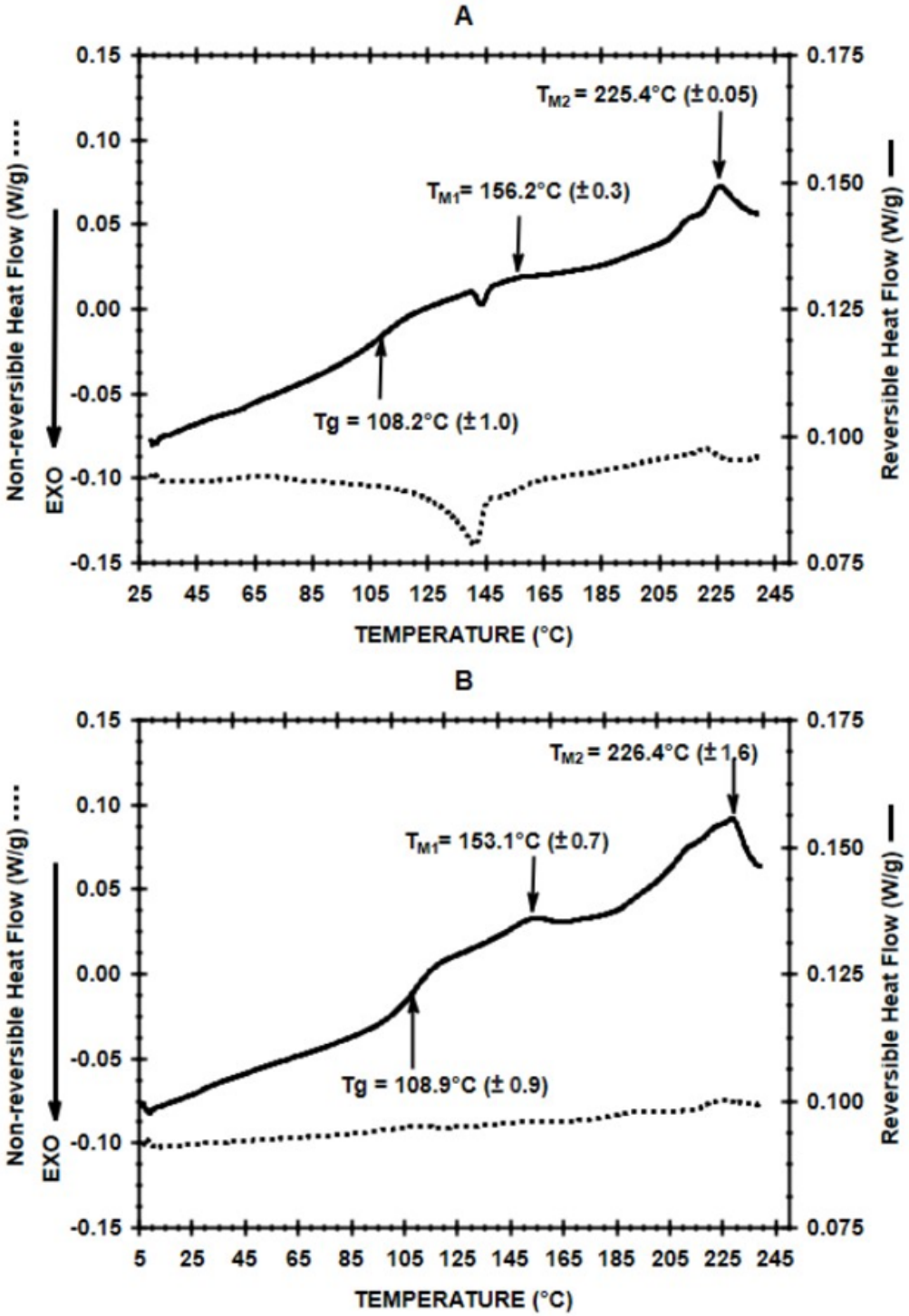

Figure 1

Thermograms for the reversing (solid line) and non-reversible (dotted line) components of the heat flow obtained from the first (A) and second (B) heating of the 4cP EC. The arrows show the Tg, T_{M1} and T_{M2} and corresponding mean and standard deviation values determined from the first (A) and second (B) heating of two independent determinations (n = 2).

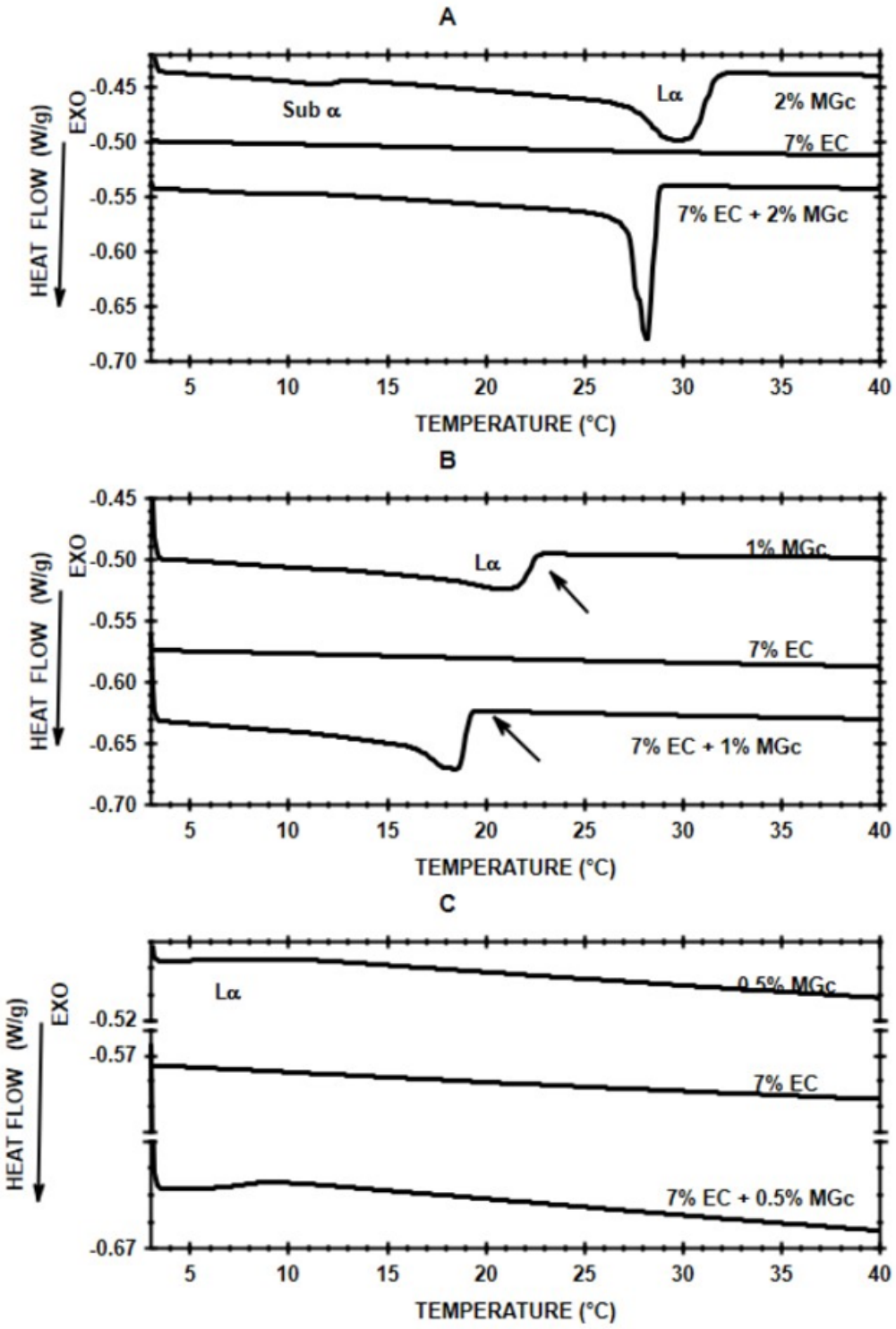

Figure 2

Cooling thermograms for the 7% EC and the 2%, 1%, and 0.5% MGc oil solutions, in comparison with the cooling thermograms for the corresponding 7% EC-2% MGc (A), 7% EC-1% MGc (B), and 7% EC-0.5% MGc (C) mixtures in the vegetable oil. As a reference, the endotherms associated with the Lα and sub-α phase transitions of the MGc are indicated.

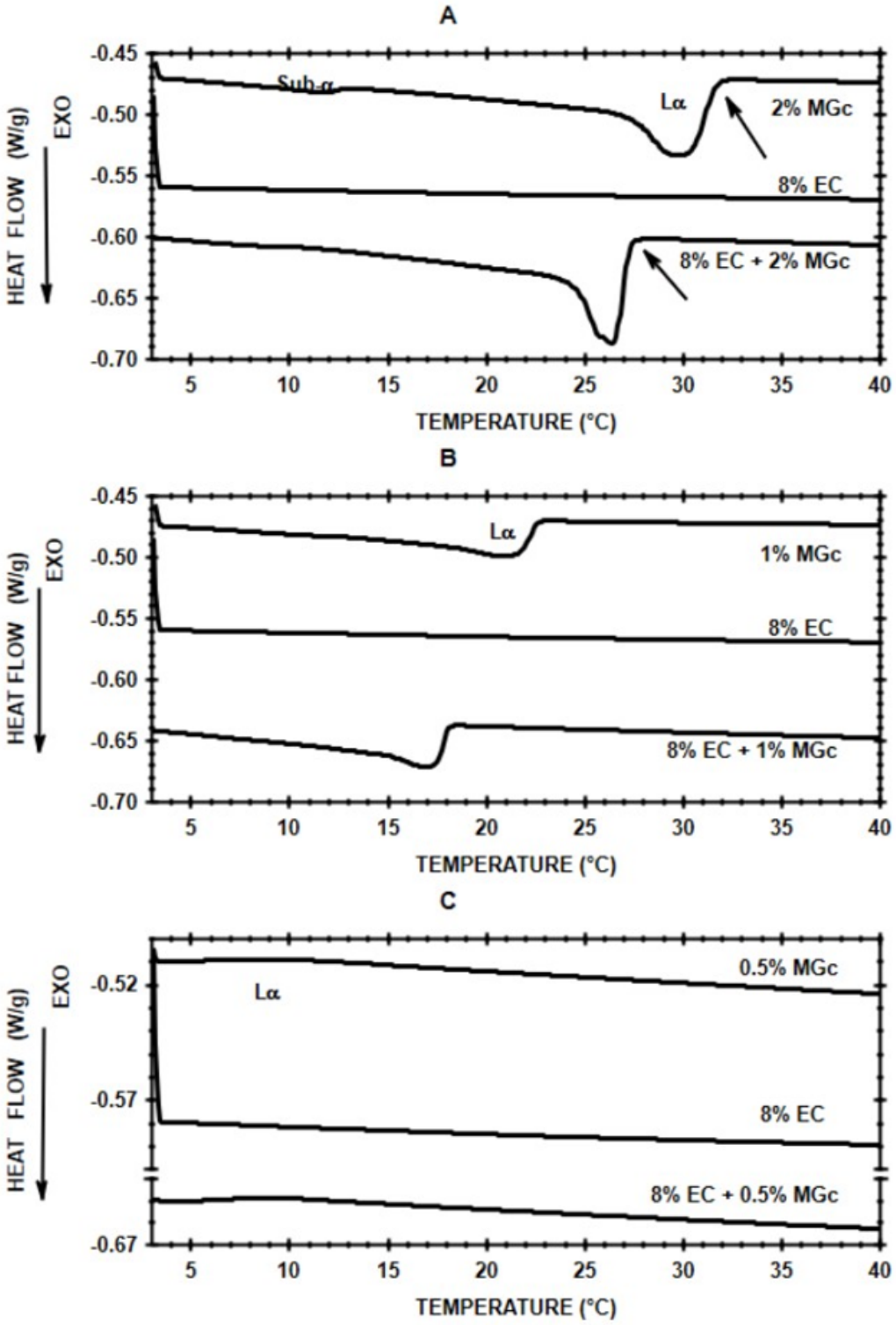

Figure 3

Cooling thermograms for the 8% EC and the 2%, 1%, and 0.5% MGc oil solutions, in comparison with the cooling thermograms for the corresponding 8% EC-2% MGc (A), 8% EC-1% MGc (B), and 8% EC-0.5% MGc (C) mixtures in the vegetable oil. As a reference, the endotherms associated with the Lα and sub-α phase transitions of the MGc are indicated.

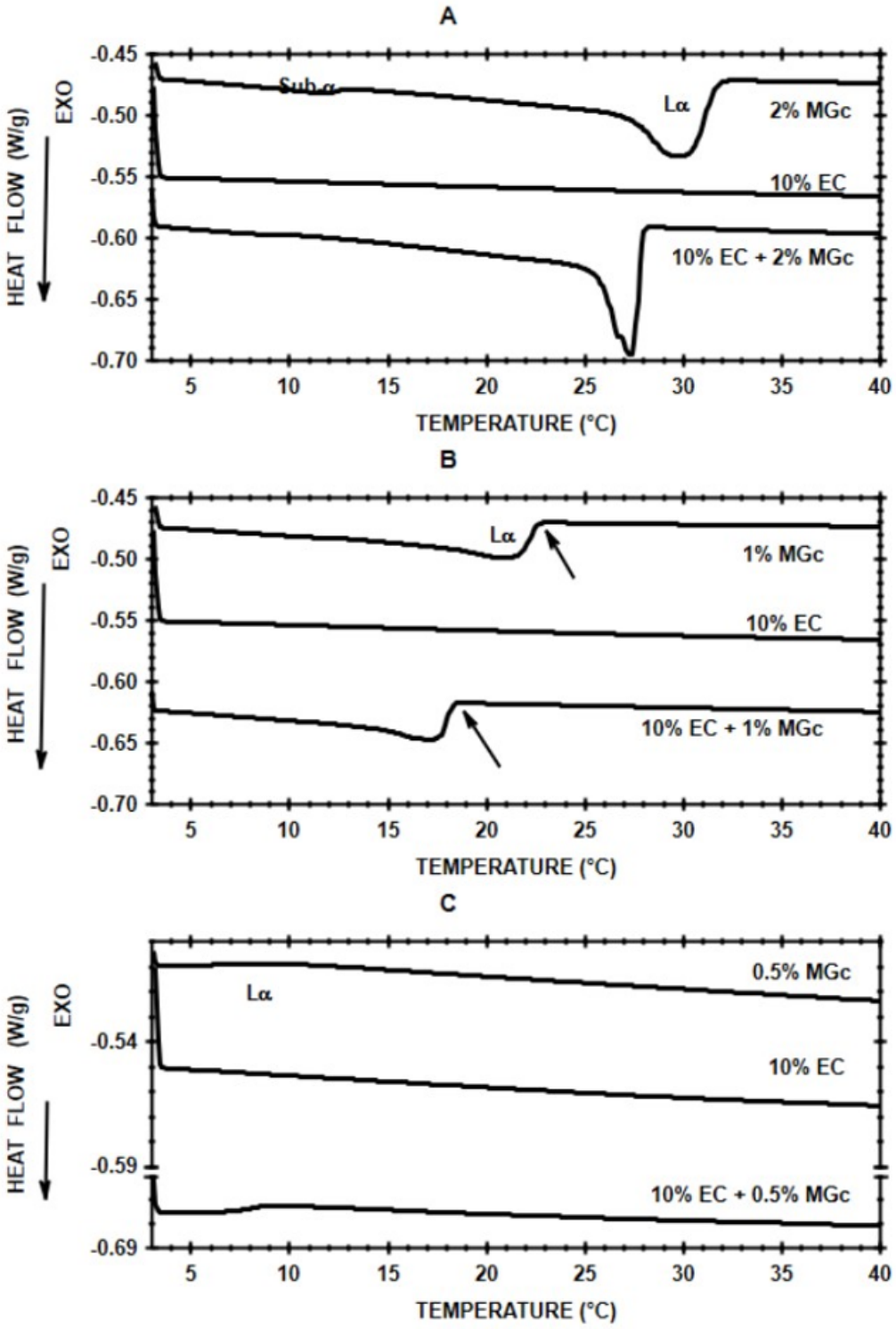

Figure 4

Cooling thermograms for the 10% EC and the 2%, 1%, and 0.5% MGc oil solutions, in comparison with the cooling thermograms for the corresponding 10% EC-2% MGc (A), 10% EC-1% MGc (B), and 10% EC-0.5% MGc (C) mixtures in the vegetable oil. As a reference, the endotherms associated with the Lα and sub-α phase transitions of the MGc are indicated.

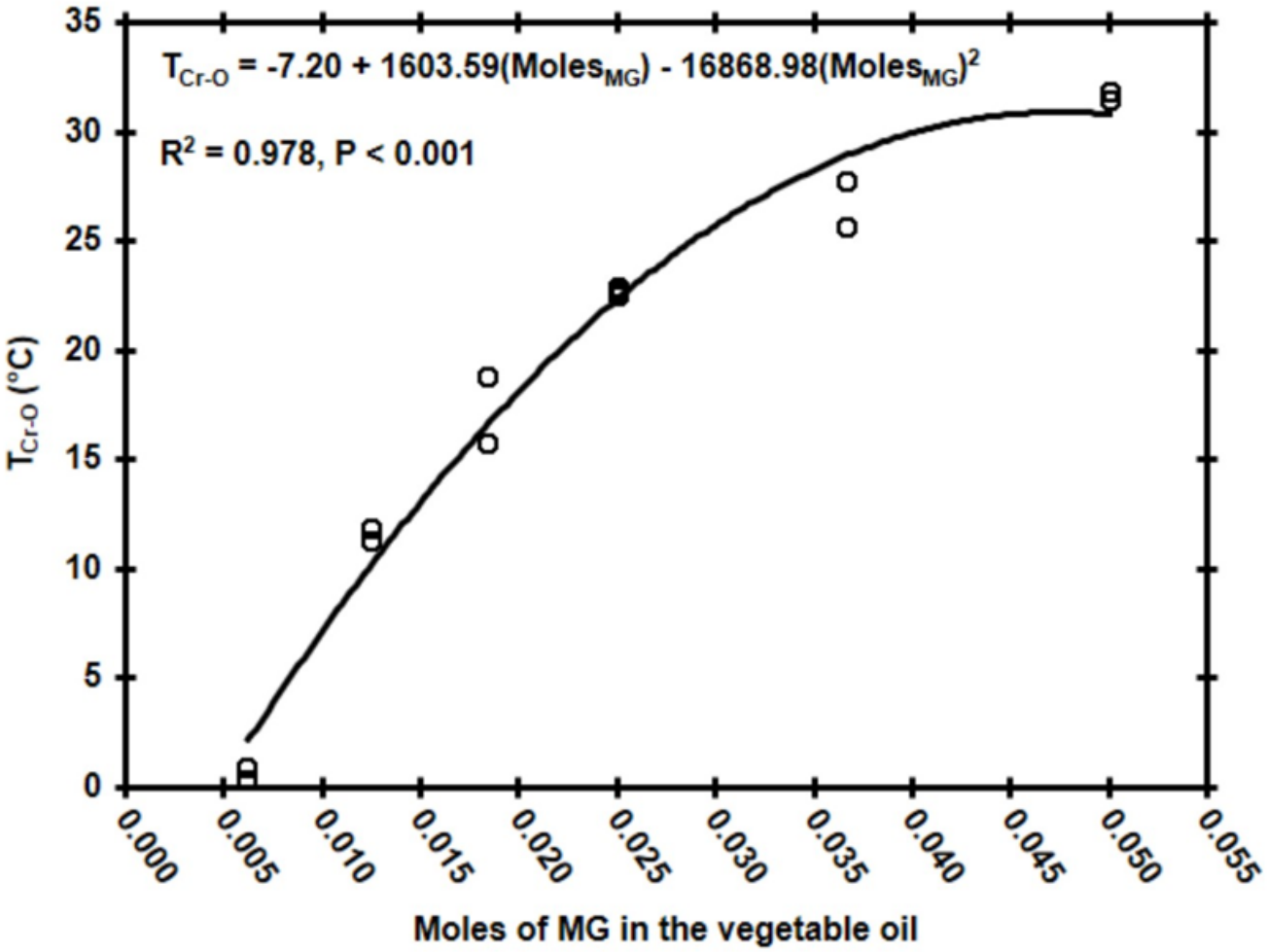

Figure 5

Behavior of the onset temperature for the Lα phase crystallization of the MGc (T_{Cr-O}) as a function of the monoglyceride (MG) concentration in the vegetable oil (corresponding to 0.25% to 2%). The regression equation of T_{Cr-O} on the MG concentration in the vegetable is included indicating the corresponding determination coefficient (R^2).

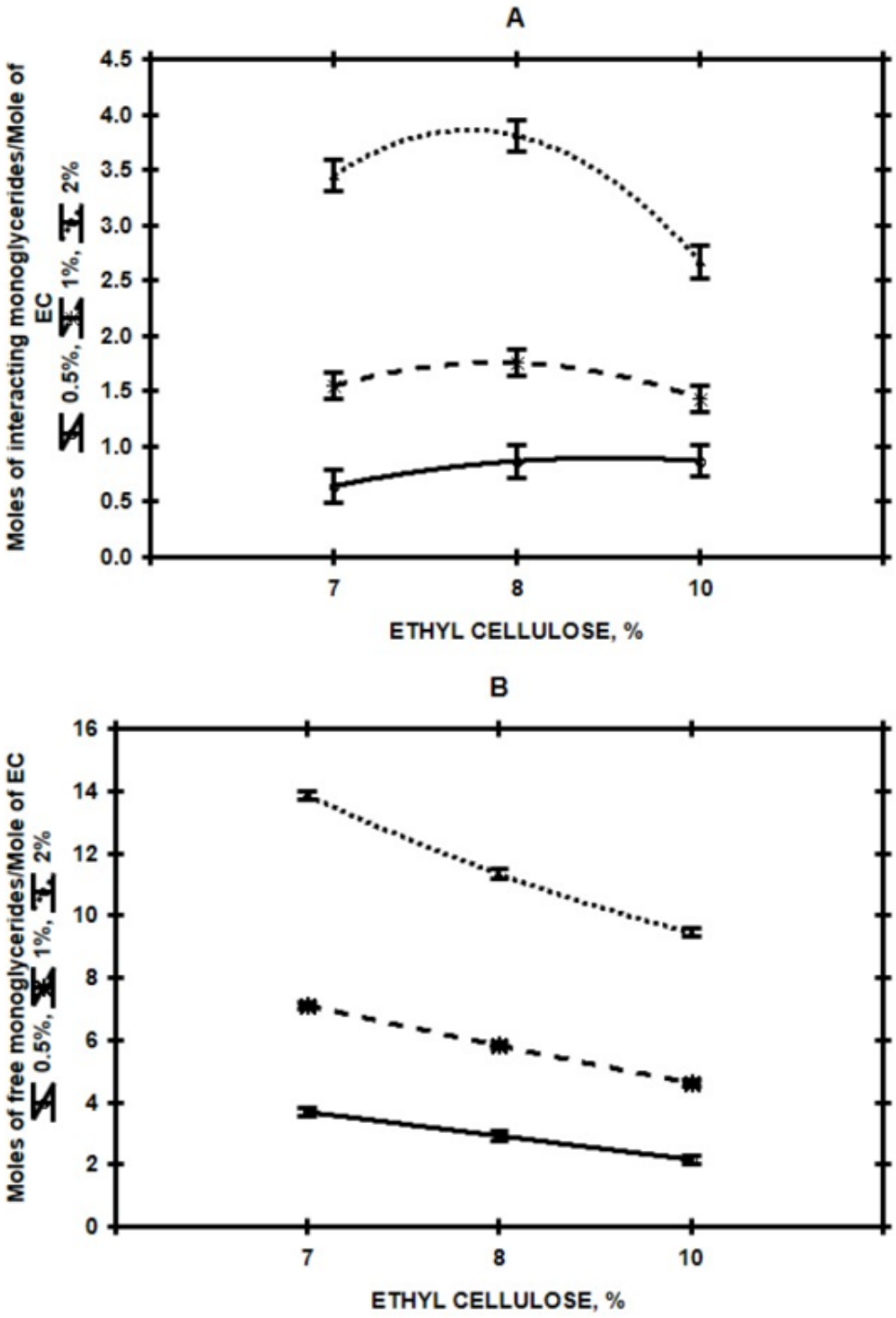

Figure 6

Concentration of monoglycerides that interacted with the EC (expressed as Moles of interacting monoglycerides/Mole of EC; insert A), and of monoglycerides remaining in the oil solution (expressed as Moles of free monoglycerides/Mole of EC; insert B) as a function of the concentration of EC and MGc (0.5%, 1.0% and 2%).

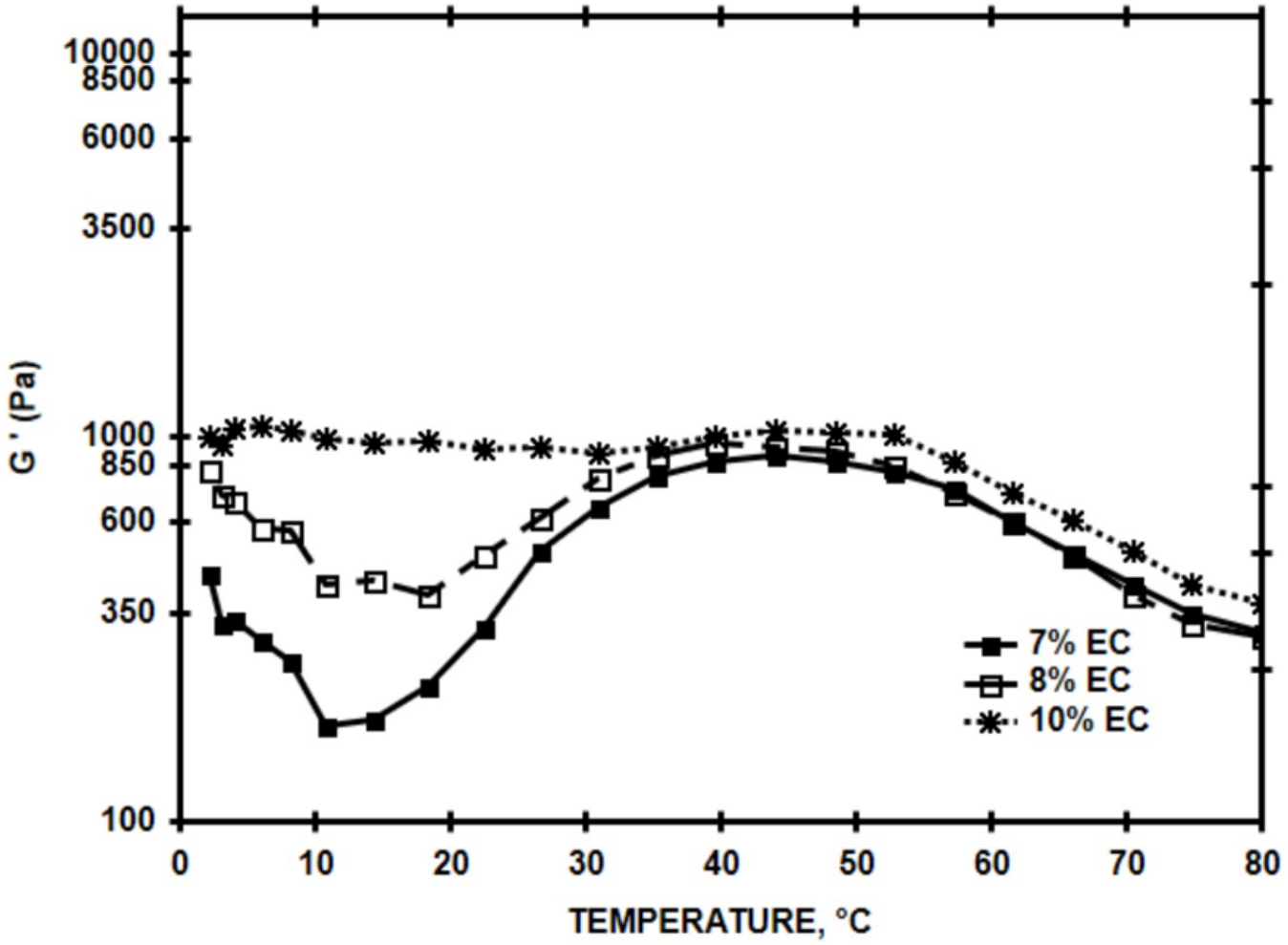

Figure 7

Behavior of the elastic modulus (G') during cooling of the 7%, 8%, and 10% EC vegetable oil solutions. The values represent G' mean values of two independent determinations with variation coefficient lower than 10%.

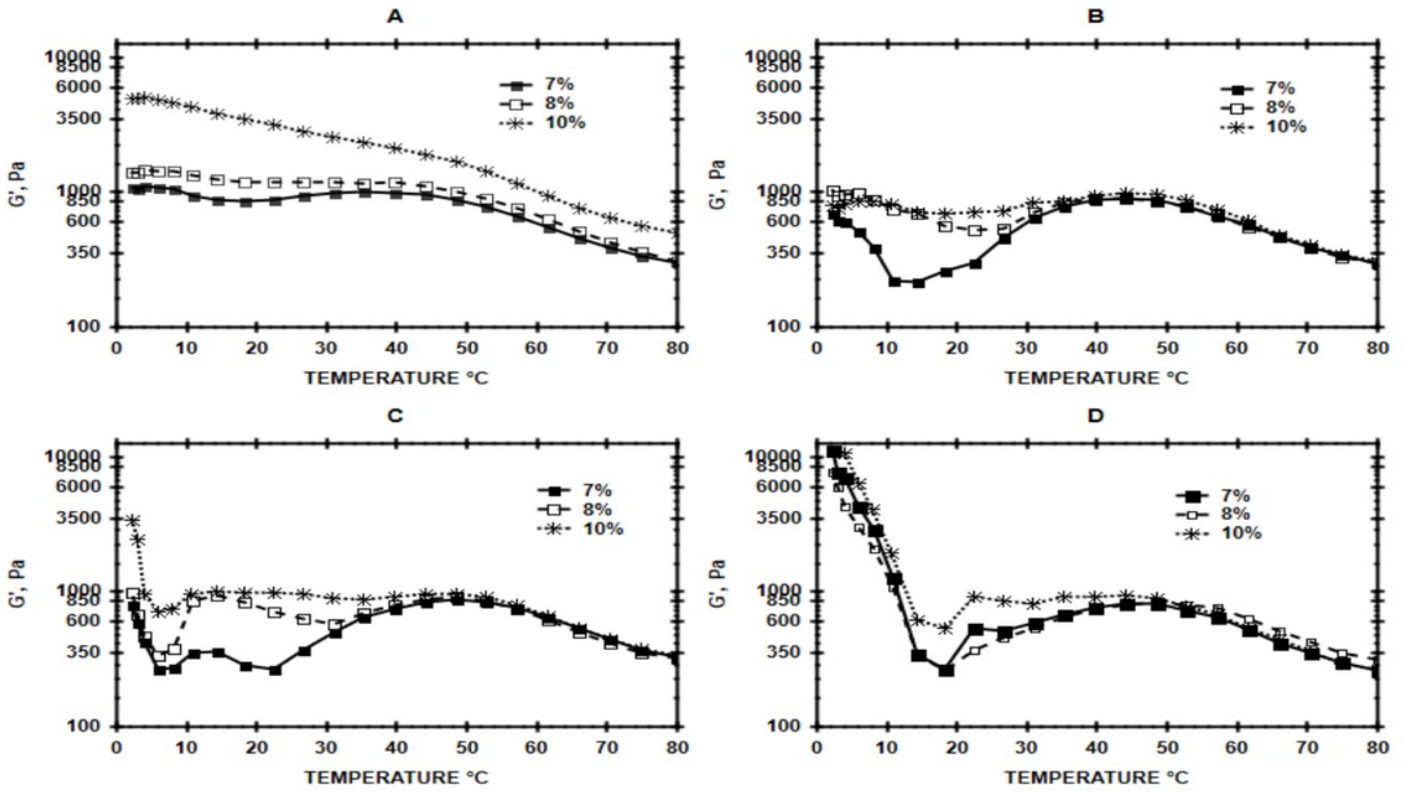

Figure 8

Behavior of the elastic modulus (G') during cooling (10°C/min) of the EC-0.10% MGc (A), EC-0.25% MGc (B), EC-0.50% MGc (C), and EC-1.0% MGc (D) systems at the different EC concentrations studied (7%, 8%, and 10%). The values represent the G' mean values of two independent determinations with variation coefficient lower than 9%.

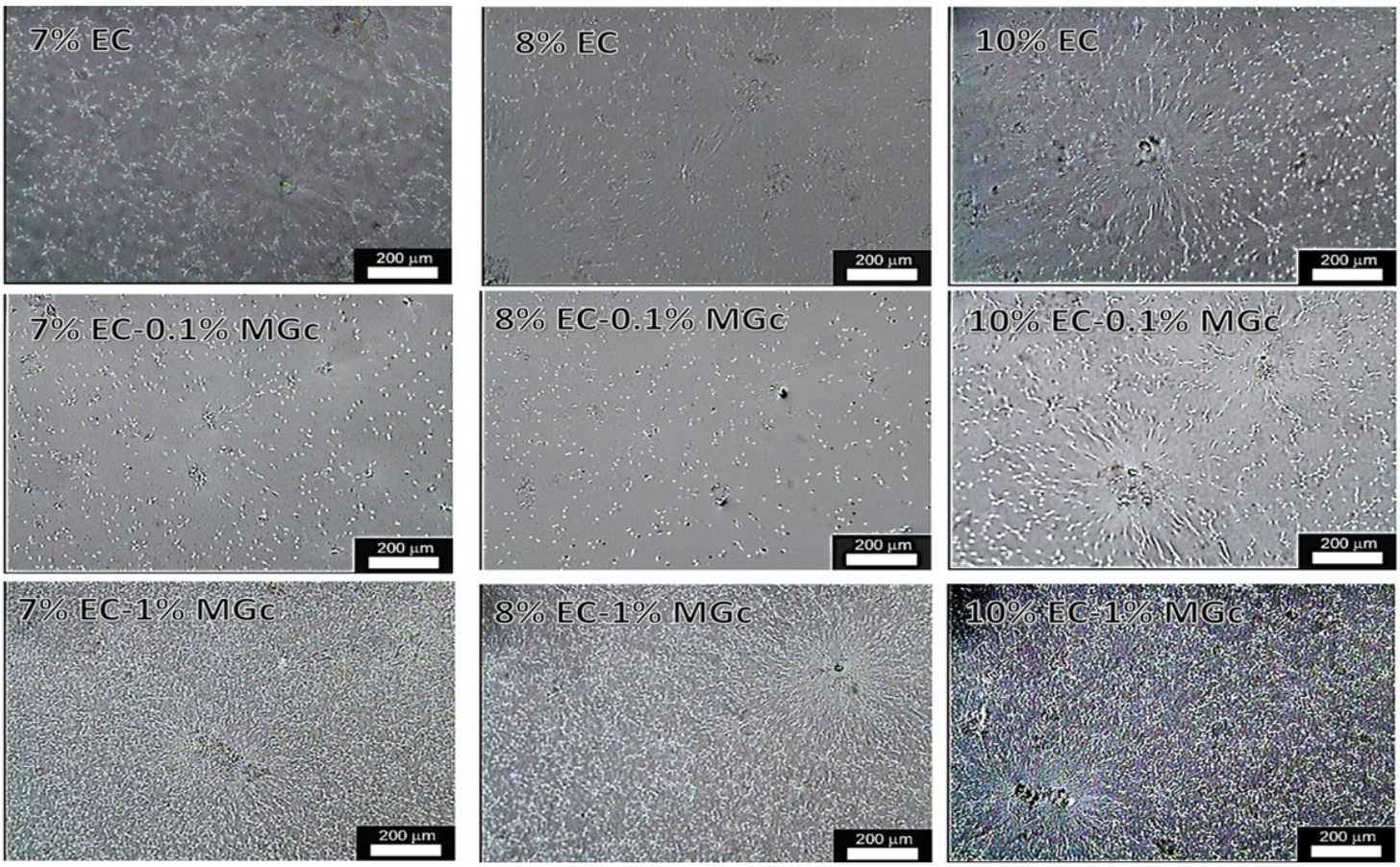

Figure 9

Photographs of the 7%, 8% and 10% EC systems in comparison with the corresponding EC-0.1% MGc and EC-1% MGc systems. The photographs were obtained at 2°C using visible light.

Supplementary Files

This is a list of supplementary files associated with this preprint. Click to download.

- SUPPLEMENTARYINFORMATIONETHYCELLULOSEMGcOct2023.pdf